Functional Materials 14, No.4 (2007)

X-ray photoelectron spectroscopy of nanopowders of ZrO_2-Y_2O_3-Cr_2O_3 compounds

A.M.Korduban[*], *I.A.Yashchishyn, T.E.Konstantinova,*
I.A.Danilenko, G.K.Volkova, V.A.Glazunova

A.Galkin Donetsk Institute for Physics and Engineering, National
Academy of Sciences of Ukraine, 72 R.Luxemburg St., 83114 Donetsk, Ukraine
[*]G.Kurdyumov Institute of Metal Physics, National Academy of Sciences
of Ukraine, 36 Acad. Vernadsky Blvd., 03680 Kyiv, Ukraine

Received July 20, 2007

The X-ray photoelectron spectroscopy investigation of doped zirconium dioxide nanopowders of ZrO_2 + 3 mol.% Y_2O_3 + 0.5 % Cr_2O_3, ZrO_2 + 0.5% Cr_2O_3 and ZrO_2 + 3 mol.% Y_2O_3 compositions has been carried out in order to obtain information about surface states of the nanoparticles. Samples of all compositions are nonstoichiometric and include four states of zirconium atoms: $Zr^{4+}(O^{2-})$, $Zr^{4+}(OH)$, Zr^{3+}, and Zr^{2+}. Although initial states of samples doped with yttrium and chromium and with yttrium only differ slightly from one another, after calcination at 600 °C in air for 1 h, intensity of component corresponding to Zr-OH bond in case of Y-doping decreased by 58% and in case of Y and Cr doping by 27% only. This fact shows that doping with chromium oxide slows down depiction of OH groups and explains nanopowders crystallization process delay.

Методом рентгеновской фотоэлектронной спектроскопии исследованы нанопорошки легированного диоксида циркония следующих составов: ZrO_2 + 3 мол.% Y_2O_3 + 0.5 % Cr_2O_3, ZrO_2 + 0.5% Cr_2O_3 и ZrO_2 + 3 мол.% Y_2O_3, для получения информации о поверхностных состояниях. Все образцы характеризуются нестехиометрией и содержат четыре состояния атомов циркония на поверхности: $Zr^{4+}(O^{2-})$, $Zr^{4+}(OH)$, Zr^{3+} и Zr^{2+}. Хотя начальные состояния образцов, легированных иттрием и хромом и только иттрием, отличаются незначительно, после прокаливания в воздушной атмосфере при 600 °C в течение 1 часа, интенсивность компоненты, соответствующей связи Zr-OH, в случае легирования Y уменьшилась на 58%, а в случае легирования Y и Cr – только на 27%. Данный факт свидетельствует о том, что легирование хромом замедляет процесс ухода OH групп и объясняет задержку кристаллизации нанопорошков при нагреве.

Doped zirconia is used widely in different fields, such as structural and functional ceramics, as catalysts, sensors, solid electrolytes of Solid Oxide Fuel Cells (SOFC), etc. In last years, a great interest is observed in nanotechnology, and in particular, in zirconia nanopowders. It is connected with the fact that with decreasing particle size down to a certain limit, the amount of surface atoms becomes comparable with amount of atoms in the bulk, thus affecting dramatically the properties of materials.

There are three polymorphs of zirconia: monoclinic (m), tetragonal (t), and cubic (c). The transformation between different polymorphs is very important for the processing and mechanical properties of zirconia ceramics. It is well known that in order to obtain stable t- or c-phase zirconia at room temperature, doping of zirconia with oxides, such as CaO, MgO, Y_2O_3, and CeO_2 is required. The crystallization process of doped zirconia is very complex and includes a phase transformation with chemical reaction. In Fig. 1, the TG, DTG, and DTA data for composition $ZrO_2 + 3$ mol.% Y_2O_3 are shown. As it is seen from the DTA data, the crystallization of doped zirconia takes place at 442°C.

Over the last years, most of publications are devoted to zirconia ceramics doped with a single oxide. Although optimized properties can be obtained in these ceramics, ternary systems on ZrO_2-base are drawing an increasing interest. Incorporation of second dopant makes it possible to improve mechanical properties, increase ionic conductivity, reduce the sintering temperature of ceramics, etc. For example, adding 1 % of Yb_2O_3 to zirconia stabilized with 1 % Y_2O_3 results in complete stabilization of tetragonal phase, while 3 % of Y_2O_3 is needed to stabilize t-phase of ZrO_2 in a binary system [1]. The influence of second element doping of Y, Ce, Sc and Ca-stabilized zirconia with such elements as Y, Ni, Fe, Cu, Mn, Al, Bi and Zn on electrical conductivity and mechanical properties of solid electrolytes are shown in [2–9]. Ce-doped yttria stabilized zirconia is one of the promising materials for nuclear waste storage due to its high mechanical properties, high radiation stability and high melting temperature [10]. Ti-doped yttria stabilized ZrO_2 appears to be an attractive material for SOFC electrodes due to its mixed conductivity [11]. Several studies of structural and mechanical properties of Y and Ce stabilized zirconia doped with Al, Mn, Fe, Nd and Yb oxides were also carried out [1, 12–15]. ZrO_2–CeO_2–CuO ternary system is investigated as catalyst for oxidation of propane and toluene [16].

In our previous studies [17–20] on the influence of second element doping on properties of stabilized zirconia nanopowders, it has been shown that chromium doping of yttria stabilized zirconia increases the crystallization temperature by more than 100°C and triggers the temperature dependence of susceptibility from diamagnetic to paramagnetic type [21]. The aim of this work was to compare the surface state of chromium doped yttria stabilized zirconia nanopowders with yttria stabilized zirconia ones. Correspondingly, X-ray photoelectron spectroscopy method was chosen to investigate surface state of hydroxide and oxide zirconia nanopowders doped by yttrium and chromium oxides.

Zirconia hydroxide nanopowders were prepared by co-precipitation technique. Aqueous solutions of $ZrO(NO_3)_2$, $Y_2(NO_3)_3$ and $CrCl_3{\cdot}6H_2O$ taken at stoichiometric ratio and mixed together were used as starting materials. This precursor solution was mixed with 25 % ammonia solution. After reaction completion, the precipitate was repeatedly water washed to remove NO_3^- ions. In this state, zirconium-yttrium hydroxide gel contained 85–90 % of water and had an amorphous structure. The precipitates were then dried in air at 120°C in a microwave oven. A 600 W magnetron served as source of microwave radiation with operating frequency of 2.45 GHz. The samples of following compositions were investigated: $ZrO_2 +$ 3 mol.% $Y_2O_3 + 0.5$ % Cr_2O_3, $ZrO_2 +$ 0.5 % Cr_2O_3 and $ZrO_2 + 3$ mol.% Y_2O_3 labeled ZYC, ZC, and ZY, respectively. The oxide nanopowders were obtained from hydroxides by calcination at 600°C in air for 1 h, and labeled as ZYCT, ZCT, and ZYT, respectively. The phase composition and average grain size (CSA) were determined by X-ray diffraction using a DRON-3 instrument at room temperature. Electron structure of nanopowders was investigated by X-ray photoelectron spectroscopy method using ES-2402 spectrometer (E $\mathrm{MgK}_\alpha = 1253.6$ eV, $P = 200$ W, $p = 2{\cdot}10^{-7}$ Pa) equipped with PHOIBOS-100 SPECS energy analyzer. The spectrometer was also equipped with an IQE-11/35 ion gun and the slow electrons gun FG-15/40 to compensate the surface charge of insulators. The Zr3d XPS spectra were decomposed into pairs of components with the following parameters $E_b(3d_{3/2}–3d_{5/2}) = 2.4$ eV, $I(3d_{3/2})/I(3d_{5/2}) = 0.66$. The Gauss-Newton method was applied in calculation. The component areas were calculated after background subtraction by Shirley method. Chemical composition, average grain size (CSA) and phases of oxide samples (labeled T) are shown in Table 1. X-ray photoelec-

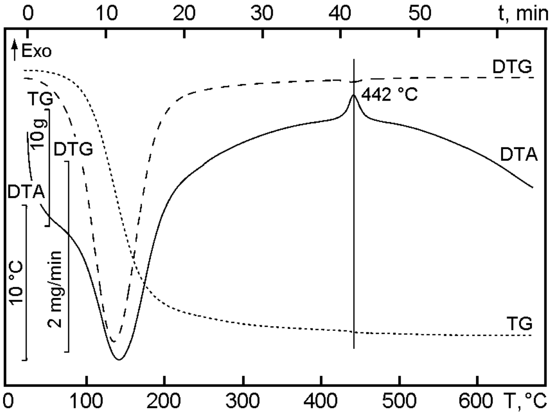

Fig. 1. TG, DTG, and DTA curves of ZrO_2 + 3 mol.% Y_2O_3.

Table 1. Labeling, chemical composition, size (CSA) and phases of zirconium oxide nanoparticles calcined at 600°C in air

Label	Composition	Grain size, nm	Phases
ZYCT	ZrO_2 + 3 mol.% Y_2O_3 + 0.5 % Cr_2O_3	11.1	100 % T
ZCT	ZrO_2 + 0.5 % Cr_2O_3	10.1	73 % T + 27 % M
ZYT	ZrO_2 + 3 mol.% Y_2O_3	15.5	100 % T

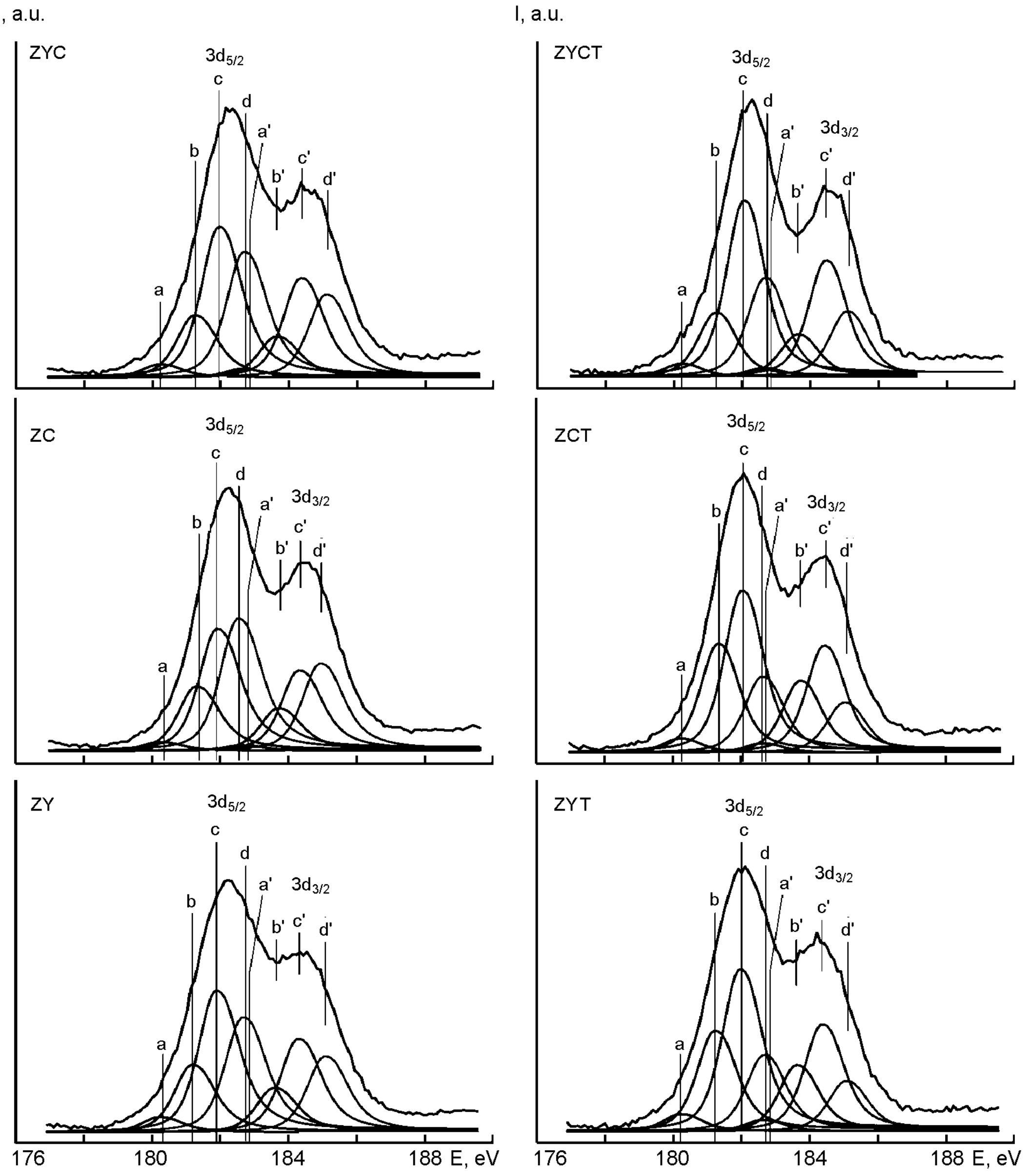

Fig. 2. XPS spectra of Zr3d levels, T — after calcination at 600°C in air; components of Zr3d$_{5/2}$ level labeled as a,b,c,d are: Zr^{2+} ($E_b3d_{5/2}$ = 180.2 eV), Zr^{3+}($E_b3d_{5/2}$ = 181.2 eV), $Zr^{4+}(O^{2-})$ ($E_b3d_{5/2}$ = 181.9 eV), Zr^{4+}(OH) ($E_b3d_{5/2}$ = 182.7 eV), respectively, components a',b',c',d' correspond to Zr3d$_{3/2}$ level.

tron spectra are shown in Fig. 2, the component intensities, in Table 2.

The X-ray diffraction results show that zirconia hydroxide powders are amorphous. The oxide species calcined at 600°C are

Table 2. Intensities of components of Zr3d- and O1s- XPS spectra

Charge state	Binding energy, eV	Relative intensity					
		ZYC	ZYCT	ZC	ZCT	ZY	ZYT
Zr^{2+}	180.2 ($3d_{5/2}$)	3.8	3.8	2.8	4.2	4.5	4.8
Zr^{3+}	181.2 ($3d_{5/2}$)	17.6	18.1	19.6	30.0	19.8	28.2
$Zr^{4+}(O^{2-})$	181.9 ($3d_{5/2}$)	42.8	50.0	37.2	44.8	41.8	45.5
Zr^{4+}(OH)	182.7 ($3d_{5/2}$)	35.7	28.1	40.4	21.0	33.9	21.5
Zr–O–Y	528.2 (O1s)	6.1	16.9	1.8	1.8	7.3	2.7
H_2O	533.0 (O1s)	8.1	2.6	3.5	3.4	5.0	1.6

100 % tetragonal, except for ZCT one which also includes 27 % of monoclinic phase. This is connected with the small amount of chromium oxide which is insufficient for complete stabilization of tetragonal phase [22]. Nevertheless, dopants with ionic radius smaller than Zr atomic radius are not referred to as stabilizers. The ZYT sample is a well studied tetragonal zirconia dioxide with crystallization temperature around 425°C, but adding 0.5 % of Cr_2O_3 induces the crystallization temperature shift towards higher temperature region by more than 100°C [17].

The surface state of hydroxide and oxide nanoparticles is complex and shows several states with different binding energies corresponding to different nonequivalent states of zirconium atoms, as it can be seen from the XPS spectra of Zr3d levels (Fig. 2). On the surface of these nanoparticles, zirconium atoms are present in four states: Zr^{2+} ($E_b3d_{5/2}$ = 180.2 eV, complex a), Zr^{3+} ($E_b3d_{5/2}$ = 181.2 eV, complex b), $Zr^{4+}(O^{2-})$ with $E_b3d_{5/2}$ = 181.9 eV, (complex c) and Zr^{4+}(OH) with $E_b3d_{5/2}$ = 182.7 eV (complex d), respectively. $Zr^{4+}(O^{2-})$ and Zr^{4+}(OH) states are common for investigated systems and presence of Zr^{3+} and Zr^{2+} states may be connected with the difference between speeds of OH groups detachment and replacement them with oxygen atoms. Zr^{2+} states were also observed by other researchers [23, 24]. In the stabilized materials, the effective reduction of the zirconium coordination by oxygen from eightfold to sevenfold results in the introduction of occupied Zr4d valence bands which are associated with Zr^{2+} [24].

The presence of Zr^{3+} states with energy $E_b3d_{5/2}$ = 181.2 eV in Zr3d spectra can be connected with non-stoichiometry of investigated oxides and hydroxides. According to [25], charge compensation under oxygen defects formation may occur in two ways, either under connection of an electron to Zr^{4+} ion with transition of the latter to the lower valence state or under electron localization in oxygen vacancy with F-center formation (detachment of OH groups requires one electron per one oxygen vacancy). The influence of Cr doping on nanoparticles system behavior was investigated in different studies by EPR method [20, 26, 27]. These investigations demonstrate possibility of use of Cr ions as markers, carrying information about properties of zirconia nanoparticles and their changes under different conditions. The significant increase of Zr^{3+} component in the case of one-element (Cr or Y) doping, in contrast to doping with two elements (Cr and Y) should be also mentioned. In the case of simultaneous doping with chromium and yttrium oxides, this fact may be associated with inhibition of OH group detachment and crystallization onset [17]. High intensity of Zr^{3+} component in comparison to traditionally observed nonstoichiometry is explained by great contribution of surface in nanopowder system. Unlike EPR spectroscopy, the XPS method discovers Zr^{2+} state, which can also be associated with surface dehydration of hydroxide and oxide nanoparticles. As it is seen from the TG curve (Fig. 1), the mass loss does not stop even above 650°C.

The doping of zirconium hydroxide and oxide affects all components of Zr3d levels, but the most dramatic effect it has on $Zr^{4+}(O^{2-})$ and Zr^{4+}(OH) states. The initial states of samples with yttrium and chromium and with yttrium only differ slightly from one another, but after calcination at 600°C for 1 h in air, amount of Zr–OH bonds in case of Cr-doping decreased by 21 % in contrast to simultaneous doping by chromium and yttrium oxides, where this value amounts 37 %. The increased amount of OH bonds in calcined sample with yttrium and chromium influences the crystallization process, also increasing the crystallization temperature by more than 100°C. The O1s states which correspond to absorbed H_2O molecules disappear almost completely after calcination for all samples. The dynamics of changes is specific for each sample, but the general trend is reduction of hydroxide states contribution, although hydroxide states do not disappear completely after calcination at 600°C. For all calcined samples, the ratio $Zr^{4+}(O^{2-})/Zr^{4+}(OH)$ of surface states increases, resulting in increased amount of oxide states. The lowest value of $Zr^{4+}(O^{2-})/Zr^{4+}(OH)$ ratio corresponds to the sample containing both yttrium and chromium dopants. Such a behavior may result from increase of M–OH complex binding energy due to presence of chromium atoms. $Zr^{4+}(O^{2-})/Zr^{4+}(OH)$ ratio for samples containing only Y and only insert space "Cr dopants" is higher than for sample including both dopants. This fact shows that the doping with second element can affect M–OH complex binding energy [20].

According to the data shown in Table 2, a change of Zr–O–Y states also takes place on the surface of nanoparticles after calcination. For sample with chromium and yttrium dopants, a considerable rise of such states occurs, contrary to the sample without chromium. This can be associated with the diffusion of yttrium atoms to the surface of particles or with partial destruction of the shell consisting of H_2O and OH molecules.

The described changes of states in doped ZrO_2 nanoparticles can impact dramatically the properties of this particulate systems, such as agglomeration, catalytic activity, sorption properties, compacting, etc.

Thus, the surface of both zirconium hydroxide and oxide has a rather complex structure and includes $Zr^{4+}(O^{2-})$, $Zr^{4+}(OH)$, Zr^{2+} and Zr^{3+} states. $Zr^{4+}(O^{2-})$ and $Zr^{4+}(OH)$ states are common for investigated systems while the presence of Zr^{3+} and Zr^{2+} states may be connected with the difference between speeds of OH groups detachment and replacement them with oxygen atoms. A high non-stoichiometry degree observed in our experiments can be explained by contribution from the surface of investigated nanoparticles.

The contribution from Zr^{4+}–OH bonds in case of simultaneous (Cr and Y) and separate (Cr or Y) doping decreases from 40.4 % to 33.9 % with maximum value in 0.5 % Cr doped zirconia sample. The use of simultaneous or separate doping makes it possible to change the non-stoichiometry degree of oxide matrix. So, in the case of simultaneous doping with chromium and yttrium, the amount of Zr^{3+} states changes after calcination only slightly (3 %), while separate doping with chromium or yttrium results in a significant increase of Zr^{3+} states by 53 % and 42 %, respectively.

Doping of zirconium hydroxide and oxide affects all components of Zr3d XPS spectra, but most dramatically influences the $Zr^{4+}(O^{2-})$ and $Zr^{4+}(OH)$ states. The amount of hydroxyl groups after calcination is much higher for sample with yttrium and chromium dopants, though initial states of samples ZrO_2 + 3 mol.% Y_2O_3 + 0.5 % Cr_2O_3 and ZrO_2 + 3 mol.% Y_2O_3 differ only slightly. This fact shows that doping with both chromium and yttrium oxides can affect the M–OH complex binding energy and explains the crystallization temperature increase by more than 100°C.

This work has been done under the project of STCU-NAS of Ukraine # 4140 and NAS of Ukraine grant # 103/07-H.

References

1. Y.Kan, G.Zhang, P.Wang et al., *J.Eur.Cer.Soc.*, **26**, 3607 (2006).
2. J.-H.Lee, S.M.Yoon, B.-K.Kim et al., *SSI*, **144**, 175 (2001).
3. C.R.Foschini, D.P.f.Souza, P.I.P.Filho et al., *J.Eur.Cer.Soc.*, **21**, 1143 (2001).
4. S.Ran, L.Winnubst, W.Wiratha et al., *J.Eur.Cer.Soc.*, **26**, 391 (2006).
5. J.V.Herle, R.Vasquez, *J.Eur.Cer.Soc.*, **24**, 1177 (2004).
6. J.-H.Lee, Y.-S.Jung, H.-S.Woo et al., *J.Eur.Cer.Soc.*, **24**, 1129 (2004).
7. M.Hirano, T.Oda, K.Ukai et al., *SSI*, **158**, 215 (2003).
8. B.A.Boukamp, T.P.Raming, A.J.A.Winnubst et al., *SSI*, **158**, 381 (2003).
9. Y. Liu, L.E. Lao, *SSI*, **177**, 159 (2006).
10. A.A.Bukaemskiy, D.Barrier, G.Modolo, *J.Eur.Cer.Soc.*, **26**, 1507 (2006).
11. K.Kowalski, A.Bernasik, J.Camra et al., *J.Eur.Cer.Soc.*, **26**, 3139 (2006).
12. T.Xu, J.Vleugels, O.Van der Biest et al., *J.Eur.Cer.Soc.*, **26**, 1205 (2006).
13. V.R.Mastelaro, V.Briois, D.P.F.de Souza et al., *J.Eur.Cer.Soc.*, **23**, 273 (2003).
14. Y.Sakka, T.Ishii, T.S.Suzuki et al., *J.Eur.Cer.Soc.*, **24**, 449 (2004).
15. S.-Y.Yang, J.-H.Lee, J.-J.Kim et al., *SSI*, **172**, 413 (2004).
16. M.Labaki, S.Siffert, J.-F.Lamonier et al., *Appl.Catal.B: Env.*, **43**, 261 (2003).
17. T.Konstantinova, I.Danilenko, A.Dobricov et al., in: Proc. of Int. Conf. on Advances in Science and Technology, Techna, 30 (2003), p.187.

18. T.E.Konstantinova, in: Proc. of Int. Conf. on Nanosize Systems: Electronic, Atomic Structure and Properties, Kiev, Ukraine (2004), p.399.
19. D.L.Savina, V.V.Tokiy, T.E.Konstantinova et al., in: Proc. Int. Conf. on Nanosize Systems: Electronic, Atomic Structure and Properties, Kiev, Ukraine (2004), p.84.
20. A.B.Brick, I.P.Bykov, M.D.Glinchuk et al., *Nanostr.Mat.Sci.*, **1**, 67 (2006).
21. K.I.Yanyshkevich, O.F.Demidenko, T.E.Konstantinova et al., *High Pres. Phys. and Techn.*, **13**, 48 (2003).
22. G.Stefanic', S.Music, A.Gajovic, *J.Mol. Struct.*, **744–747**, 541 (2005).
23. C.Diagne, H.Idriss, K.Pearson et al., *Compt. Rend. Chim.*, **7**, 617 (2004).
24. R.H.French, S.J.Glass, F.S.Ohuchi et al., *Phys.Rev.B*, **49**, 8, 5133 (1994).
25. V.N.Strecolovskiy, Yu.M.Polezaev, S.F.Palguev, Oxides with Impurity Caused Disorder, Composition, Structure, Phase Transformations, Nauka, Moskva, (1987) [in Russian].
26. A.M.Slipenyuk, M.D.Glinchuk, I.P.Bykov, *Ferroelectrics*, **298**, 289 (2004).
27. A.B.Brick, I.P.Bykov, M.D.Glinchuk et al., *Nanostr.Mat.Sci.*, **1**, 91 (2005).

Рентгенівська фотоелектронна спектроскопія нанопорошків складу ZrO_2-Y_2O_3-Cr_2O_3

О.М.Кордубан, І.О.Ящишин, Т.Є.Константінова, І.А.Даніленко, Г.К.Волкова, В.О.Глазунова

Методом рентгенівської фотоелектронної спектроскопії досліджено нанопорошки легованого діоксиду цирконію наступних складів: ZrO_2 + 3 мол.% Y_2O_3 + 0.5 % Cr_2O_3, ZrO_2 + 0.5% Cr_2O_3 та ZrO_2 + 3 мол.% Y_2O_3 з метою отримання інформації про поверхневі стани. Всі зразки характеризуються нестехіометрією та містять чотири стани атомів цирконію на поверхні: $Zr^{4+}(O^{2-})$, $Zr^{4+}(OH)$, Zr^{3+} та Zr^{2+}. Початковий стан зразків, легованих ітрієм та хромом та тільки ітрієм, практично не відрізняється, але після відпалу при 600 °C впродовж 1 години інтенсивність компоненти, що відповідає зв'язку Zr-OH у випадку легування Y зменшилась на 58%, а у випадку легування Y та Cr – тільки на 27%. Цей факт вказує на те, що легування хромом уповільнює процес відриву OH груп та пояснює затримання кристалізації нанопорошків при відпалі.